Biochimie 94 (2012) 2673–2680

Contents lists available at SciVerse ScienceDirect

Biochimie

journal homepage: www.elsevier.com/locate/biochi

Research paper

Ultrafast electron transfer in riboflavin binding protein in macromolecular crowding of nano-sized micelle

Surajit Rakshit, Ranajay Saha, Pramod Kumar Verma, Rajib Kumar Mitra, Samir Kumar Pal*

Department of Chemical, Biological and Macromolecular Sciences, S.N. Bose National Centre for Basic Sciences, Block JD, Sector III, Salt Lake, Kolkata 700098, India

ARTICLE INFO

Article history:
Received 17 June 2012
Accepted 6 August 2012
Available online 21 August 2012

Keywords:
Molecular and macromolecular crowding
Electron transfer in riboflavin binding protein in cellular environments
Picosecond-resolved electron transfer dynamics of Vitamin B_2 in protein
Ligand binding in micellar crowding
Tertiary structure of riboflavin binding protein

ABSTRACT

In this contribution, we have studied the dynamics of electron transfer (ET) of a flavoprotein to the bound cofactor, an important metabolic process, in a model molecular/macromolecular crowding environments. Vitamin B_2 (riboflavin, Rf) and riboflavin binding protein (RBP) are used as model cofactor and flavoprotein, respectively. An anionic surfactant sodium dodecyl sulfate (SDS) is considered to be model crowding agent. A systematic study on the ET dynamics in various SDS concentration, ranging from below critical micellar concentration (CMC), where the surfactants remain as monomeric form to above CMC, where the surfactants self-assemble to form nanoscopic micelle, explores the dynamics of ET in the model molecular and macromolecular crowding environments. With energy selective excitation in picosecond-resolved studies, we have followed temporal quenching of the tryptophan residue of the protein and Rf in the RBP–Rf complex in various degrees of molecular/macromolecular crowding. The structural integrity of the protein (secondary and tertiary structures) and the vitamin binding capacity of RBP have been investigated using various techniques including UV–Vis, circular dichroism (CD) spectroscopy and dynamic light scattering (DLS) studies in the crowding environments. Our finding suggests that the effect of molecular/macromolecular crowding could have major implication in the intra-protein ET dynamics in cellular environments.

1. Introduction

The detailed knowledge of the biophysical and biochemical reaction has traditionally been acquired through experiments conducted in buffer solutions containing low concentrations of biomolecules together with low molecular weight substrates, and cofactors as required, assuming the representation of the in vivo scenario. In contrast, the real biological environment differs from that idealized solvent bath in different aspects. Such as the intracellular environment is highly crowded because of the presence of large amounts of soluble and insoluble biomolecules, including proteins, nucleic acids, ribosomes, lipids and carbohydrates, etc [1–4]. This means that a significant fraction of the intracellular space is not available to other macromolecular species, as a result of this, macromolecular thermodynamic activities increase by several orders of magnitude. Therefore, biochemical reaction in a living cell may be quite different from those under idealized conditions [5]. In this sense, it is highly demanding to understand the effects of the crowding agents, termed "macromolecular crowding" [6,7], on biophysical and biochemical reaction. Although the effect of macromolecular crowding, in particular on proteins in vitro with regard to folding and denaturation, has been well studied [8–13] less is known about the biochemical reactions. One such biochemical reaction is electron transfer (ET), which plays an important role in many processes in chemistry, physics and biology and has diverse technological applications. In biological systems, ET reactions are ubiquitous [14,15] especially in enzymes with redox reactions [16]. Flavoproteins with flavin chromophores are examples of such enzymes and are involved in various catalytic processes [17–19]. The understanding of ET reactions of flavins in proteins and their redox reactions is critical to their functionality. In this report we have studied ET dynamics of riboflavin (Rf; vitamin B_2) in Rf binding protein (RBP), a globular monomeric protein and is responsible for the storage and active transport of riboflavin cofactor into developing embryo [20,21], also important for their functions as photoreceptors, in the presence of crowding environment of nanoscopic sodium dodecyl sulfate (SDS) micelles.

Abbreviations: ET, electron transfer; Rf, riboflavin; RBP, riboflavin binding protein; SDS, sodium dodecyl sulfate; CMC, critical micellar concentration; CD, circular dichroism; DLS, dynamic light scattering; Trp, tryptophan; IRF, instrument response function; TCSPC, time-correlated single-photon counting; FRET, Förster resonance energy transfer; GndHCl, guanidium hydrochloride; d_h, hydrodynamic diameter; R_0, Förster distance.

* Corresponding author. Tel.: +91 33 2335 5705/6/7/8; fax: +91 33 2335 3477.
E-mail address: skpal@bose.res.in (S.K. Pal).

0300-9084/$ – see front matter © 2012 Elsevier Masson SAS. All rights reserved.
http://dx.doi.org/10.1016/j.biochi.2012.08.005

Although ET between Rf and RBP in dilute homogeneous aqueous solution has been studied quite thoroughly [22–25], much less is known about ET between Rf and RBP under crowded environments. Remarkably, crowded environment often alters the structure and functionality of many proteins. Biological function of a protein is possible only when it is folded into a specific three-dimensional conformation. An understanding of the mechanisms of ET involving in crowded environments provides an important bridge between commonly employed dilute solutions in vitro studies and studies of the effects of a crowded environment, as found in vivo. The anionic surfactant sodium dodecyl sulfate (SDS) is often used to mimic cellular membrane and macromolecular crowding agent [26] and is used here as model crowding agent. Importance of using SDS as model crowding agent lies on the following facts. At a concentration below the critical micellar concentration (CMC; 3.3 mM in buffer), SDS essentially remains in monomeric form and expected to mimic molecular crowding. Above CMC the SDS molecules form well-defined spherical micelles (4.4 nm diameter) comparable to the size of RBP (4.7 nm), and mimic the macromolecular crowding environments. It has also to be noted that, SDS is well known to act as a potential denaturants in their monomeric form [27], thus the use of the SDS surfactant as potential crowding agent is expected to mimic the cellular complex environment complicated by both chemical denaturant and molecular/macromolecular crowding agent.

In the present report, we have explored picosecond-resolved dynamics of both RBP and Rf in the RBP–Rf complex under various degrees of molecular/macromolecular crowding. While selective excitation (300 nm) and detection at 350 nm explores the dynamics of the ET from the tryptophan in the proximity of the cofactor Rf, the excitation of the complex at 445 nm (detection at 520 nm) clearly reveals the dynamics of ET of the cofactor Rf in the crowded environment. We have also monitored the effect of structural perturbation (both secondary and tertiary) of RBP on the observed ET dynamics using near- and far-UV circular dichorism (CD), dynamic light scattering (DLS) and UV–Vis spectroscopy of the bound cofactor Rf.

2. Materials and methods

2.1. Materials and sample preparation

Riboflavin binding protein (RBP; Apo form) from chicken egg white (lyophilized powder) and L-tryptophan (L-Trp) were purchased from Sigma. Sodium dodecyl sulfate (SDS; Fluka), disodium hydrogen phosphate dehydrate (Sigma 99%), and sodium dihydrogen phosphate dehydrate (Sigma 99%) were used as received. Aqueous stock solutions of RBP were prepared in a phosphate buffer (10 mM) at pH 7.0 using double distilled water.

2.2. UV–visible absorption spectroscopy

Concentration of RBP in buffer was determined using the extinction coefficient value of 49,000 $M^{-1}\,cm^{-1}$ at 280 nm. Riboflavin (Rf) concentration was calculated from its absorbance using the extinction coefficient value of 12,200 $M^{-1}\,cm^{-1}$ at 450 nm. Unless otherwise mentioned, we have used 15 μM RBP and 7.5 μM Rf solutions for all the spectroscopic studies.

2.3. Circular dichroism spectroscopy

Far-, near-, and visible-UV circular dichroism (CD) measurements were performed on a JASCO 815 spectrometer. Far-UV CD studies were measured between 200 and 260 nm wavelength with protein concentration of 0.15 mg ml^{-1} using a cell of 0.1 cm path length. Both near-UV and visible–UV CD measurements were made in 1.0 cm path length cell.

2.4. Steady-state absorption and fluorescence spectroscopy and DLS measurements

Absorption and emission spectra were recorded with a Shimadzu UV-2450 spectrophotometer and a JobinYvon Fluoromax-3 fluorimeter, respectively. DLS measurements were made with Nano-S Malvern instrument employing a 4 mW He–Ne laser ($\lambda = 632.8$ nm) with protein concentration of 5 mg ml^{-1} and concentration ratio of SDS and RBP was maintained similar to that of absorption and fluorescence studies.

2.5. Time-resolved fluorescence spectroscopy

We used a commercially available picosecond diode laser-pumped (LifeSpec-ps) time-resolved fluorescence spectrophotometer from Edinburgh Instruments, U.K. for time-resolved measurement. For 445 nm excitation, a diode laser was used with instrument response function (IRF) of 80 ps. For RBP, we have used a femtosecond-coupled TCSPC (time-correlated single-photon counting) setup in which the sample was excited by the third harmonic laser beam (300 nm) of the 900 nm (0.5 nJ per pulse) using a mode-locked Ti-sapphire laser with an 80 MHz repetition rate (Tsunami, Spectra Physics), pumped by a 10 W Millennia (Spectra Physics) followed by a pulse-peaker (rate 8 MHz) and a third harmonic generator (Spectra Physics, model 3980). The third harmonic beam was used for excitation of the sample inside the TCSPC instrument (IRF = 70 ps) and the second harmonic beam was collected as for the start pulse. Luminescence transients were fitted by using a commercially available software F900 (LifeSpec-ps) from Edinburgh Instruments, U.K. using a nonlinear least square fitting procedure to a function ($X(t) = \int_0^t E(t')R(t-t')\mathrm{d}t'$) comprising of convolution of the IRF ($E(t)$) with a sum of exponentials ($R(t) = A + \sum_{i=1}^{N} B_i e^{-t/\tau_i}$) with pre-exponential factors (B_i), characteristic lifetimes (τ_i) and a background (A). Relative concentration in a multiexponential decay was finally expressed as; $a_n = (B_n/\sum_{i=1}^{N} B_i) \times 100$.

To estimate the Förster resonance energy transfer (FRET) efficiency of the donor (tryptophan) and hence to determine the distance of the donor–acceptor pair, we followed the Förster formalism [28]. The Förster distance (R_0) is given by,

$$R_0 = 0.211\left[\kappa^2\, n^{-4} Q_D J(\lambda)\right]^{1/6} \quad \left(\text{in } \text{Å}\right) \tag{1}$$

where κ^2 is a factor describing the relative orientation in space of the transition dipoles of the donor and acceptor (Rf). For donor and acceptors that randomize by rotational diffusion prior to energy transfer, the magnitude of κ^2 is assumed to be 2/3. In the present study the same assumption has been made. The refractive index (n) of the medium is assumed to be 1.4. Q_D, the quantum yield of the tryptophan in the donor protein (RBP) in the absence of acceptor, is measured to be 0.06. $J(\lambda)$, the overlap integral, which expresses the degree of spectral overlap between the donor emission and the acceptor absorption is given by,

$$J(\lambda) = \frac{\int_0^\infty F_D(\lambda)\varepsilon(\lambda)\lambda^4 \mathrm{d}\lambda}{\int_0^\infty F_D(\lambda)\mathrm{d}\lambda} \tag{2}$$

where $F_D(\lambda)$ is the fluorescence intensity of the donor in the wavelength range of λ to $\lambda + \mathrm{d}\lambda$ and is dimensionless. $\varepsilon(\lambda)$ is the extinction coefficient (in $M^{-1}\,cm^{-1}$) of the acceptor at λ. If λ is in

nm, then $J(\lambda)$ is in units of $M^{-1}\,cm^{-1}\,nm^4$. Once the value of R_o is known, the donor–acceptor distance (r) can easily be calculated using the formula,

$$r^6 = \frac{\left[R_0^6(1-E)\right]}{E} \tag{3}$$

here E is FRET efficiency. The energy transfer efficiency is measured from the lifetime values of the donor, in absence and presence of the acceptor (τ_D and τ_{DA}, respectively).

$$E = 1 - \left(\frac{\tau_{DA}}{\tau_D}\right) \tag{4}$$

It has to be noted that Eq. (4) holds rigorously only for a homogeneous system (i.e. identical donor–acceptor complexes) in which the donor and the donor–acceptor complex have single exponential decays. However, for donor–acceptor systems decaying with multiexponential lifetimes, FRET efficiency (E) is calculated from the amplitude weighted lifetimes $\langle\tau\rangle = \sum \alpha_i\tau_i$ where α_i is the relative amplitude contribution to the lifetime τ_i. We have used the amplitude weighted time constants for τ_D and τ_{DA} to evaluate E using Eq. (4).

3. Results and discussions

Fig. 1A and B shows the steady-state (insets) and picosecond-resolved fluorescence decay transients of tryptophan ($\lambda_{ex} = 300$ nm, fluorescence decay monitored at 350 nm) and Rf ($\lambda_{ex} = 445$ nm, fluorescence decay monitored at 520 nm), respectively, of RBP–Rf complex in the presence of increasing amount of crowding agent SDS. Earlier studies have concluded that RBP quenches the fluorescence of Rf which is a consequence of ultrafast ET to the flavin chromophore (Rf) in the excited electronic state from nearby tryptophan or tyrosine residues present in RBP. It has also been shown that complexation of Rf with RBP quenches both the fluorescence of Rf and Trp of the protein [23,24]. It is observed that addition of SDS to RBP–Rf complex leads to a recovery of Trp emission as well as that of Rf (insets of Fig. 1A and B). It is interesting to note that Rf absorbs mostly ~450 nm, however, it shows distinct absorbance in the 300 nm region. When RBP–Rf complex in buffer is excited at 300 nm, no emission peak in the 520 nm region is observed. However, as SDS is gradually added in the complex, a distinct peak at ~520 nm appears and its intensity increases with the addition of SDS (inset of Fig. 1A) and at high SDS concentrations the emission spectra resembles that of free Rf. The increase of Rf emission intensity with gradual addition of SDS is due to the expulsion of Rf from the ligand binding site of RBP, thereby hindering the ET process. Fig. 1C shows the relative fluorescence intensities of Trp of RBP–Rf complex at 350 nm and Rf of RBP–Rf complex at 520 nm at different SDS concentrations. Fig. 1C (inset) depicts the relative fluorescence intensity of Trp in RBP itself as a function of SDS concentrations. It is observed that fluorescence intensity increases with the addition of SDS, whereas that of Rf changes only marginally at all studied SDS concentrations (data not shown).

Now to get a better insight into the ET dynamics and extent of interaction of protein with crowding agent and the observed changes in fluorescence intensity, picosecond-resolved fluorescence measurements of these systems are performed. Fig. 1A shows fluorescence decay transients of Trp in RBP–Rf complex at 350 nm in buffer (circle), 1 mM SDS (triangle) and 40 mM SDS (square) excited at 300 nm. Fluorescence decay of Trp residue of RBP in buffer is fitted tri-exponentially having time components of 0.14, 0.87, and 2.88 ns with average lifetime ($<\tau>$) of 0.82 ns (Table 1).

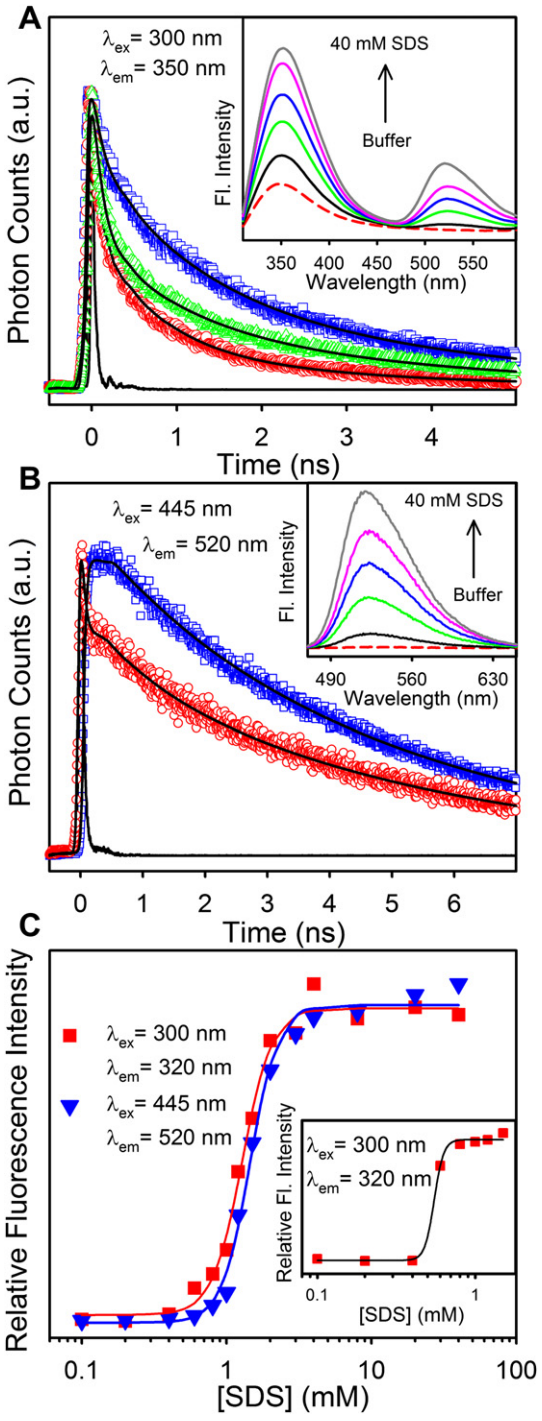

Fig. 1. (A) Fluorescence decay transients of tryptophan of RBP–Rf complex ($\lambda_{ex} = 300$ nm, decay monitored at 350 nm) in buffer (red; circle), 1 mM SDS (green, triangle) and 40 mM SDS (blue; square). The total emission spectrum of the RBP–Rf complex at different SDS concentration is shown in the inset ($\lambda_{ex} = 300$ nm). (B) Fluorescence decay transient of Rf in RBP–Rf complex ($\lambda_{ex} = 445$ nm; decay monitored at 520 nm) in 0.2 mM SDS (red; circle) and 40 mM SDS (blue; square). The total emission spectrum of the RBP–Rf complex at different SDS concentration is shown in the inset ($\lambda_{ex} = 445$ nm). (C) Relative fluorescence intensity of trp ($\lambda_{em} = 350$ nm) and Rf ($\lambda_{em} = 520$ nm) of RBP–Rf complex at different SDS concentrations (square; $\lambda_{ex} = 300$ nm, emission monitored at 350 nm and triangle; $\lambda_{ex} = 445$ nm, emission monitored at 520 nm). Inset shows the relative fluorescence intensity of RBP ($\lambda_{ex} = 300$ nm, emission monitored at 350 nm) at different concentration of SDS. (For interpretation of the references to colour in this figure legend, the reader is referred to the web version of this article.)

Table 1
Average lifetimes ($<\tau>$) of RBP, and RBP–Rf complex in buffer and different concentrations of SDS.

[SDS] (mM)	Average lifetime, $<\tau>$ (ns)		
	($\lambda_{ex} = 300$ nm; $\lambda_{em} = 350$ nm)		($\lambda_{ex} = 445$ nm; $\lambda_{em} = 520$ nm)
	RBP	RBP–Rf	RBP–Rf
0.0	0.98	0.43	0.64
0.2	0.80	0.58	1.38
0.4	0.93	0.62	2.01
0.6	1.22	0.70	3.97
0.8	1.76	0.85	4.49
1.0	1.84	0.91	4.69
1.5	1.93	1.28	4.68
2.0	1.95	1.48	4.66
3.0	1.94	1.64	4.66
4.0	1.79	1.74	4.67
8.0	1.80	1.83	4.66
20.0	1.75	1.86	4.68
40.0	1.77	1.79	4.68

On subsequent addition of the SDS, $<\tau>$ increases up to 2.0 mM SDS concentration (below CMC) beyond which it does not change appreciably (Table 1). This indicates that SDS monomer significantly alters the ET dynamics as a molecular crowding agent. It is important to note here that Trp in aqueous solution has a distinct average lifetime of 2.8 ns whereas a single Trp protein HSA (human serum albumin) has an average lifetime of 5.8 ns [29]. The lifetime of tryptophan in proteins varies from a few hundred picoseconds to 9 ns [29]. It is widely believed that the large variation in its lifetime stems from the proximity of quenching groups like glutamic acid, aspartic acid, serine, threonine, methionine, arginine etc in the vicinity of the Trp [29]. A quenched average lifetime of 0.82 ns for Trp in RBP indicates the presence of nearby quenching amino acid residues such as glutamic acid, serine and arginine, which is also evident from the high resolution X-ray crystallographic studies of RBP [30]. Addition of a molecular crowding agent like SDS releases the fluorescence quenching and as a result lifetime of Trp increases (Fig. 1 and Table 1). Previously, it has been observed that binding of SDS near Trp of BSA as well as HSA leads to the Trp fluorescence quenching and consequently decrease in lifetime of Trp [31]. It was proposed that the quenching is static in case of HSA whereas both static and dynamic in case of BSA [31]. However, the present study reveals an opposite trend, i.e., quenching is released, which rules out a direct interaction between the crowding agent and Trp. In case of RBP–Rf complex increase in $<\tau>$ (Table 1) and fluorescence intensity of Trp (inset of Fig. 1A) are due to the removal of neighbouring quencher amino acid residues and Rf form the ligand binding domain of RBP. At low SDS concentrations $<\tau>$ of Trp residue in RBP–Rf complex is smaller compared to that in RBP. However, beyond 4 mM SDS where RBP loses its vitamin binding capacity completely (discussed later), $<\tau>$ remains practically unchanged for both RBP and RBP–Rf complex.

It has been concluded that in ET process the fluctuation of the donor–acceptor distance also results in a change of the fluorescence lifetime [32]. Time-resolved florescence measurements provide with an estimation of the ET rate constant of $1.35 \times 10^9\ s^{-1}$ for RBP–Rf complex in buffer. Upon addition of SDS, ET rate constant decreases and at 0.8 mM SDS it is found to be $9.5 \times 10^6\ s^{-1}$. Beyond this SDS concentration ET eventually stops. A low ET rate constant ($10^6\ s^{-1}$) implies a distance of ~20 Å between the isoalloxazine ring (Rf) and Trp-156 (RBP) which is much larger compared to the native distance of ~3.7 Å in the absence of SDS [30,32]. This indicates that the observed decrease in vitamin binding capacity as well as inefficient ET process in presence of SDS is due to perturbation of protein structure as induced by the crowding agent. To understand this in more detail, we monitor the structure of RBP using circular dichroism (CD) technique. Fig. 2A shows the far-UV CD spectra of RBP–Rf complex in absence and presence of SDS in 200–260 nm wavelength windows. As observed from Fig. 2 and Table 2, addition of SDS molecules increases the helicity of the protein at the expense of a decrease in the percentage of random coil. Similar trend in the far-UV CD spectrum of RBP is also observed when SDS is added to RBP (data not shown). It should be noted here that the change in the helical content is most significant at a concentration below CMC (2.0 mM) (Table 2) beyond which the effect is minimal. It appears that low concentration of SDS (below CMC) acts as molecular crowder which functionally strengthen the protein's secondary structure. Such low

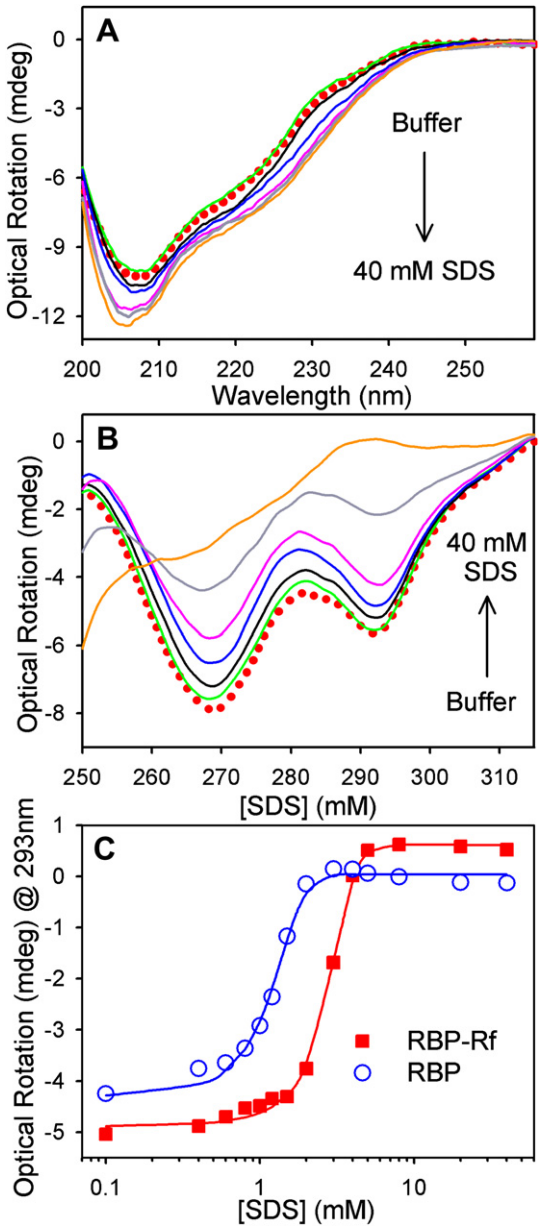

Fig. 2. (A) Far-UV CD spectra of RBP–Rf complex at various concentrations of SDS. (B) Near-UV CD spectra of RBP–Rf complex at different concentrations of SDS. (C) Optical rotation of RBP (at 293 nm; triangle) and RBP–Rf (at 293 nm; square) at different concentrations of SDS.

Table 2
Percentages of α-helix, β-structure and random coil of RBP; RBP–Rf complex in buffer and in different concentrations of SDS.

System	α-helix (%)	Anti-parallel (%)	Parallel (%)	β turn (%)	Random coil (%)
RBP	27.5	11.1	9.8	18.5	33.1
RBP + RF	27.8	11.2	9.7	18.8	32.5
0.2 SDS	27.2	11.3	9.9	18.7	32.9
0.4 SDS	29.2	10.9	9.4	18.6	31.9
0.6 SDS	29.8	10.7	9.3	18.5	31.7
0.8 SDS	28.4	10.9	9.6	18.5	32.6
1.0 SDS	30.6	10.4	9.1	18.5	31.4
1.2 SDS	30.8	10.5	9.1	18.4	31.2
1.5 SDS	32.2	10.1	8.8	18.4	30.5
2.0 SDS	32.9	9.9	8.7	18.3	30.2
3.0 SDS	32.5	10.0	8.7	18.5	30.3
4.0 SDS	32.1	10.3	8.9	18.6	30.1
5.0 SDS	33.5	9.9	8.5	18.3	29.8
8.0 SDS	33.8	9.8	8.5	18.4	29.5
20.0 SDS	32.4	10.2	8.7	18.4	30.3
40.0 SDS	33.4	9.9	8.6	18.4	29.7

SDS concentrations are incapable of forming an aggregate of the RBP polypeptide (see DLS measurement). Thus the protein structure must be stabilized by a specific function, probably a "cross-linking function" of the bound SDS as suggested by Markus et al. [33].

Near-UV CD spectrum of protein explores contribution from aromatic amino acid residues and reveals the tertiary structure of proteins. The observed near-UV CD spectrum of RBP–Rf in buffer shows a distinct peak at 268 nm along with a shoulder in the 290 nm region (Fig. 2B). The signal around 268 nm originates from tyrosine, whereas that in the 290 nm region is due to the tryptophan (Trp) residue of the protein. With gradual addition of SDS to RBP–Rf complex, the intensity of signal around 268 and 290 nm regions get reduced. As the concentration of added SDS goes beyond 3 mM the CD spectrum gets significantly distorted. The change in the 268 nm regions signifies perturbation to tyrosine, whereas that in the 290 nm regions indicates a drastic change in the Trp containing domain which is consistent with the steady-state and time-resolved studies. The protein itself also losses its tertiary structure in the presence of SDS (Fig. 2C). However, the loss of tertiary structure of RBP occurs at ~3 mM SDS in the presence of Rf and ~1.5 mM SDS in the absence of Rf (Fig. 2C). This suggests that Rf bound RBP has enhanced stability against molecular crowding environment compared to RBP itself. This is in agreement with the steady-state emission measurement where transition point for denaturation is higher for RBP–Rf complex compared to RBP without Rf (Fig. 1C). Previously it was found that Rf binding renders enhanced thermal stability of RBP, as manifested by a change in the denaturation temperature from 60.8 °C for RBP to 72.8 °C for RBP–Rf complex [34]. Loss in tertiary structure of the protein results in the expulsion of the vitamin from the binding site of RBP as evident from visible CD and absorption measurement (discussed in next paragraph). Rf either in buffer or in SDS does not show any appreciable optical activity in visible region. However upon binding with RBP, a set of strong CD bands appear in the visible region as shown in Fig. 3A. The band positioned at ~445 nm is due to the $\pi \rightarrow \pi^*$ transition, whereas those at 370 nm and 340 nm are attributed to a second $\pi \rightarrow \pi^*$ and $n \rightarrow \pi^*$ transitions, respectively [35]. These strong CD bands suggest that Rf is rigidly packed in the binding cleft and rotation of the ribose moiety is completely hindered. With increasing concentration of SDS, the CD signals in visible region get weaker and eventually disappear above ~3 mM SDS indicating the loss of binding capacity of the protein (Fig. 3B). Further confirmation

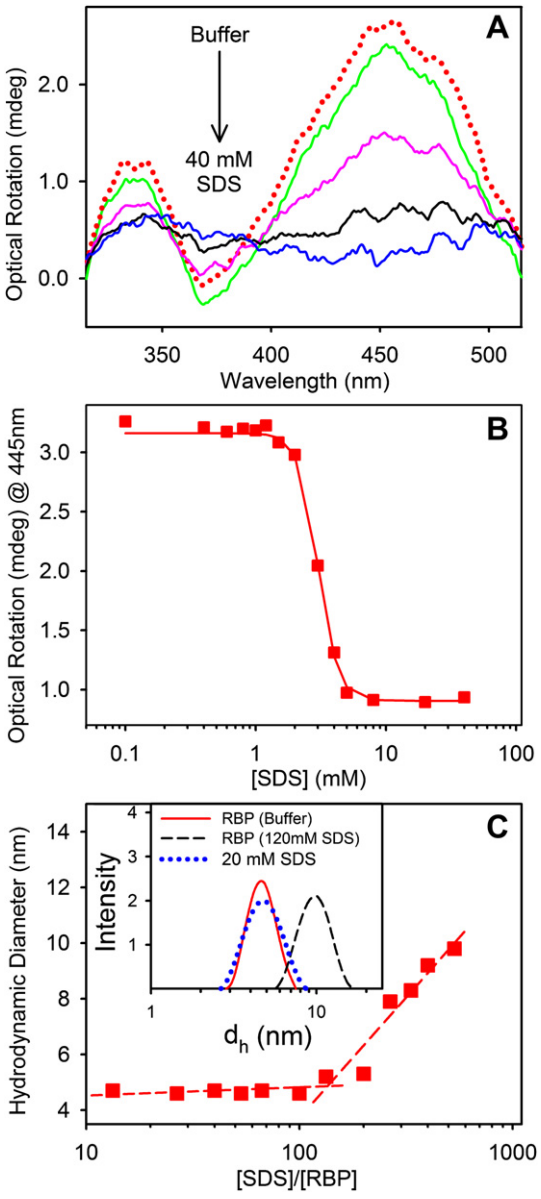

Fig. 3. (A) Visible CD spectra of RBP–Rf complex at various concentrations of SDS. (B) Optical rotation values at 445 nm of RBP–Rf complex at various concentrations of SDS. (C) Hydrodynamic diameter of RBP at different SDS concentrations. Broken lines are guide to eye. Typical DLS signals for 20 mM SDS, RBP in buffer and 120 mM SDS concentration are shown in the inset.

comes from the absorption spectra of RBP–Rf complex in the presence of different concentration of SDS (Fig. 4). It is evident from the figure 4A, C that addition of SDS leads to a considerable blue shift of the absorption maximum. The shoulder at ~490 nm which is characteristic of Rf binding progressively disappears forming an isobestic point at ~473 nm indicating the loss of vitamin binding capacity of RBP (Fig. 4A). To get a clear picture of the disappearance of the 490 nm peak we deconvolute the absorption spectra (Fig. 4B). RBP–Rf complex shows three absorption peak whereas in presence of 40 mM SDS RBP–Rf complex has only two maxima confirming the loss of binding capacity of vitamin in crowded environments.

To check whether the loss of tertiary structure of RBP as evidenced from near-UV CD is due to its unfolding, we perform DLS measurement. Inset of Fig. 3C depicts the DLS measurements of SDS

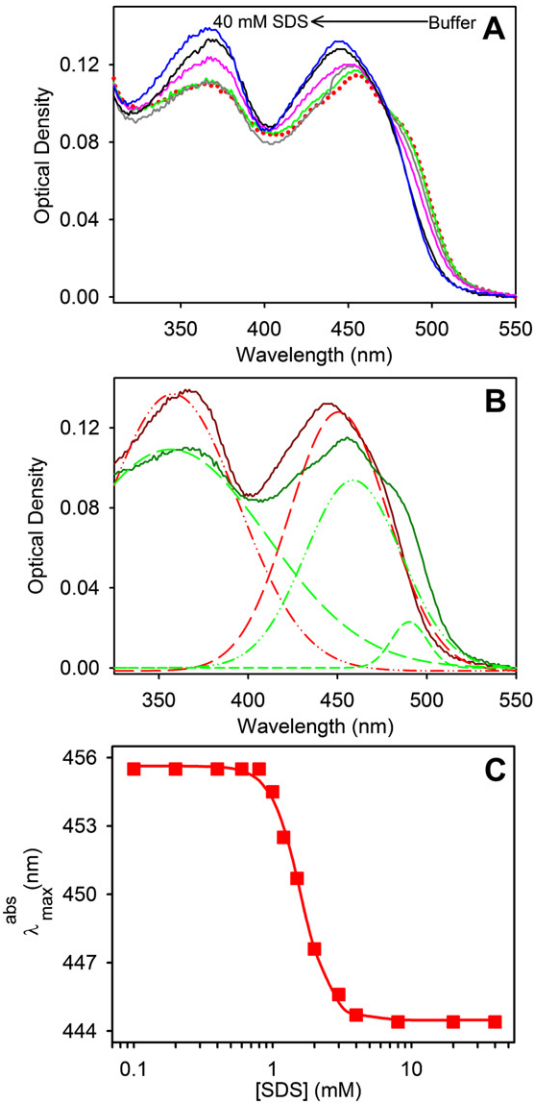

Fig. 4. (A) Absorption spectra of RBP–Rf complex at different concentrations of SDS. (B) The deconvolution of absorption spectra of RBP–Rf complex at two different SDS concentrations (0 mM (green) and 40 mM (red)). (C) The shift in absorption peak of Rf in RBP–Rf complex as a function of SDS concentrations. (For interpretation of the references to colour in this figure legend, the reader is referred to the web version of this article.)

micelle; RBP in buffer and RBP in the presence of SDS. As evident from the figure, hydrodynamic diameter (d_h) of RBP in buffer is comparable to that of SDS micelle. Thus we could not get both the peaks (protein and micelle) individually. Fig. 3C shows the change in the hydrodynamic diameter of RBP at different SDS concentrations. As evident from the figure, hydrodynamic diameter of RBP in buffer is 4.7 nm which increases to 5.2 nm at ~2 mM SDS concentration and afterwards the size increases linearly with increasing SDS concentration. Practically there is no change in the size of RBP before CMC which supports the "cross linking hypothesis" as discussed earlier. Thus the interaction of SDS and RBP is found to be weak and only with [SDS]/[RBP] ≥ 130 the protein starts unfolding (Fig. 3C). As large excess of SDS (in the form of micelles) is needed to initiate the unfolding, the interaction between SDS and RBP is assumed to be nonspecific in nature. Some other proteins like Cardiotoxin exhibits similar resistance [36], while a number of other water-soluble proteins are easily denatured by SDS [37,38]. The observed weak interaction might be due to the acidic nature of RBP which holds an overall negative charge at physiological pH. Thus excess of SDS as micellar crowding agent is needed to initiate the hydrophobic interaction with the protein interior and consequent unfolding of the protein. Since RBP unfolds in the presence of excess of SDS and losses its tertiary structure as well as its vitamin binding capacity while there is an insignificant change in secondary structure, it seems that it adopts an intermediate structure in the presence of SDS. Previous studies by Alen et al. on guanidium hydrochloride (GndHCl) denaturation of RBP concluded that the unfolding process consists of two steps with two transitions (i.e., a three-state model) and possibility of an intermediary molten globule state [39]. Further confirmation to this fact comes from spectroscopic measurements. It has been shown earlier that tryptophan emission of RBP suffers 10–12 nm red shifts on complete denaturation indicating the exposure of Trp from the interior of the protein towards a more polar aqueous environment [24,39]. In the present study, however, we find that tryptophan residue of RBP does not show any peak shift even at the highest concentration of SDS used (40 mM) either in the absence or in the presence of Rf. This affirms that SDS denatures RBP partially to an intermediate molten globular state in which RBP retains almost all of its secondary structure, however, loses its tertiary structure which in turn is unable to hold Rf and hence stops ET between the protein and vitamin.

Quenching of RBP florescence upon Rf binding has commonly been believed to be a result of efficient Förster resonance energy transfer (FRET) from excited Trp to Rf [24]. Based on the overlap of protein fluorescence and Rf absorption Li et al. calculated the Förster's parameter R_0 to be 3 Å [24]. However, Choi et al. suggested that the quenching of RBP fluorescence upon binding of Rf is due mainly to the ground-state stacking interaction between a tryptophan residue at the binding site and the quinoxaline portion of Rf, and not due to FRET [40]. The crystal structure of RBP is not available in pdb data bank which refrains us from calculating the exact distance of each Trp from Rf. However, the distance of five Trp varies from 4 to 12 Å approximately as calculated from the distances provided by Monaco et al [30]. Based on the overlap of protein fluorescence and Rf absorption and assuming random orientation of acceptor and donor dipoles and taking quantum yield of the tryptophan in the protein RBP to be 0.06, we calculate Förster distance (R_0) to be 23 Å. The energy transfer efficiency is found to be ~56% using Eq. (4). The distance between Trp and Rf is calculated to be 22 Å which is considerably higher than the acceptable distance of 4–12 Å. In order to find out whether there is possibility of energy transfer from L-Trp molecule to Rf, we perform steady-state as well as time-resolved experiment. It is important to mention here that the concentration of Rf (acceptor) is higher than that of L-Trp (donor) and also is equal to the micellar concentration. Although there is a huge quenching of L-Trp steady-state emission in buffer as well as in 40 mM SDS (inset of Fig. 5B, C respectively), the lifetime of tryptophan does not suffer any change in these systems (Fig. 5). This clearly indicates that the quenching is static in nature. Thus possibility of FRET between L-Trp and Rf is ruled out. However, both steady-state and time-resolved measurement of tryptophan residue of RBP–Rf complex (Table 1) shows quenching indicating that quenching is not completely static in case of RBP–Rf complex as suggested by Choi et al. [40]. It is important to note that both static and dynamic quenching require molecular contact between the fluorophore and the quencher. Also a distance of 4–12 Å between tryptophan residue of RBP and Rf molecule indicates a low possibility of FRET between them since for efficient FRET the donor–acceptor distance must be within 0.5 R_0 to 1.5 R_0 [41]. Based on these experimental findings we suggest that quenching of protein fluorescence upon Rf binding might be either static or combined dynamic and static but not due to FRET.

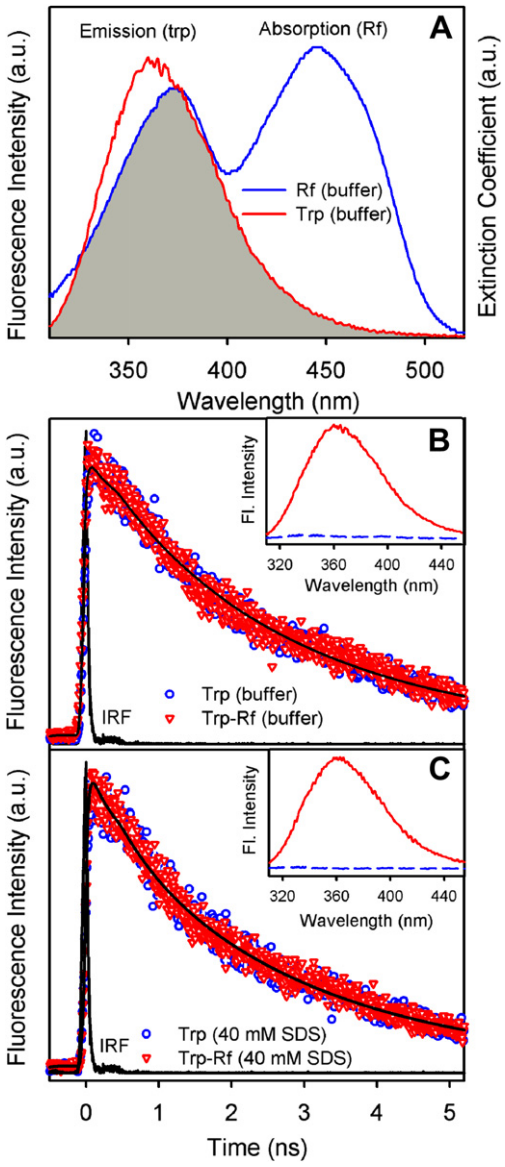

Fig. 5. (A) Spectral overlap of fluorescence emission of L-tryptophan and absorption spectrum of Rf in buffer. (B) Fluorescence decay transients of L-tryptophan ($\lambda_{ex} = 300$ nm) in the absence and presence of Rf in buffer. Corresponding steady-state emission spectra are shown in the inset. (C) Fluorescence decay transients of L-tryptophan ($\lambda_{ex} = 300$ nm) in the absence and presence of Rf in 40 mM SDS. Corresponding steady-state emission spectra are shown in the inset.

However, the detailed description of quenching is out of the scope of the present work.

4. Conclusions

In this article, we have provided an experimental evidence of the effects of molecular/macromolecular crowding in the biochemical reaction by using a simple model system. We have studied ultrafast ET dynamics of Rf in RBP. For molecular/macromolecular crowding agent we have used SDS surfactant. It has been found that the extent of ultrafast electron transfer (ET) between Rf and RBP decreases with the addition of SDS molecules. Beyond 1 mM SDS concentration ET eventually stops as revealed from picosecond-resolved fluorescence measurement indicating loss of vitamin binding capacity of RBP. We have confirmed that the secondary structure of RBP strengthens in presence of molecular crowding agents due to cross-linking. However, its tertiary structure collapses in the presence of SDS as observed from CD measurements. These observations indicate that the loss of binding capacity of RBP above 1.5 mM of SDS (below CMC where SDS exists as monomer) concentration is due to collapse of its tertiary structure. These characteristics also indicate that in presence of crowding environments RBP changes from native (N) to a molten globular like intermediate state (I) which retains its secondary structure but loses its tertiary structure. We also suggest that quenching of tryptophan emission of RBP in presence of Rf is not due to FRET as established previously rather a combination of dynamic and static quenching. Hence, our results suggest that ET rate from tryptophan(s) to Rf in the RBP in vivo is slower, considering that the intracellular milieu is crowded in nature.

Acknowledgements

S.R. and. P.K.V. thank CSIR, India, for the fellowships. We thank DST, India, for a financial Grant (SR/SO/BB-15/2007).

References

[1] E.R. John, Macromolecular crowding: obvious but underappreciated, Trends Biochem. Sci. 26 (2001) 597–604.
[2] Alice B. Fulton, How crowded is the cytoplasm? Cell 30 (1982) 345–347.
[3] S.B. Zimmerman, S.O. Trach, Estimation of macromolecule concentrations and excluded volume effects for the cytoplasm of *Escherichia coli*, J. Mol. Biol. 222 (1991) 599–620.
[4] R.J. Ellis, A.P. Minton, Cell biology: join the crowd, Nature 425 (2003) 27–28.
[5] A.P. Minton, How can biochemical reactions within cells differ from those in test tubes? J. Cell Sci. 119 (2006) 2863–2869.
[6] Allen P. Minton, Macromolecular crowding, Curr. Biol. 16 (2006) R269–R271.
[7] S.B. Zimmerman, A.P. Minton, Macromolecular crowding: biochemical, biophysical and physiological consequences, Annu. Rev. Biophys. Biomol. Struct. 22 (1993) 27–65.
[8] B. van den Berg, R. Wain, C.M. Dobson, R.J. Ellis, Macromolecular crowding perturbs protein refolding kinetics: implications for folding inside the cell, EMBO J. 19 (2000) 3870–3875.
[9] B. van den Berg, R.J. Ellis, C.M. Dobson, Effects of macromolecular crowding on protein folding and aggregation, EMBO J. 18 (1999) 6927–6933.
[10] V.N. Uversky, E.M. Cooper, K.S. Bower, J. Li, A.L. Fink, Accelerated α-synuclein fibrillation in crowded milieu, FEBS Lett. 515 (2002) 99–103.
[11] N. Tokuriki, M. Kinjo, S. Negi, M. Hoshino, Y. Goto, I. Urabe, T. Yomo, Protein folding by the effects of macromolecular crowding, Protein Sci. 13 (2004) 125–133.
[12] A. Christiansen, Q. Wang, A. Samiotakis, M.S. Cheung, P. Wittung-Stafshede, Factors defining effects of macromolecular crowding on protein stability: an in vitro/in silico case study using cytochrome c, Biochemistry 49 (2010) 6519–6530.
[13] D. Tsao, N.V. Dokholyan, Macromolecular crowding induces polypeptide compaction and decreases folding cooperativity, Phys. Chem. Chem. Phys. 12 (2010) 3491–3500.
[14] D.N. Beratan, J.N. Onuchic, Protein electron transfer, Bios Scientific Publishers, Oxford, 1996.
[15] Electron transfer in chemistry, Wiley-VCH, Weinheim, Germany, 2001.
[16] Comprehensive biological catalysis: a mechanistic reference, Academic Press, San Diego, 1998.
[17] Chemistry and biochemistry of flavoenzymes, CRC Press, Boca Raton, FL, 1991.
[18] V. Massey, The chemical and biological versatility of riboflavin, Biochem. Soc. Trans. 28 (2000) 283–296.
[19] Flavins and flavoproteins, Agency for Scientific Publishers, Berlin, 1999.
[20] W.P. Winter, E.G. Buss, C.O. Clagett, R.V. Boucher, The nature of the biochemical lesion in avian renal riboflavinuria – II. The inherited change of a riboflavin-binding protein from blood and eggs, Comp. Biochem. Physiol. 22 (1967) 897–906.
[21] C.V. Murty, P.R. Adiga, Pregnancy suppression by active immunization against gestation-specific riboflavin carrier protein, Science 216 (1982) 191–193.
[22] D.P. Zhong, A.H. Zewail, Femtosecond dynamics of flavoproteins: charge separation and recombination in riboflavine (vitamin B-2)-binding protein and in glucose oxidase enzyme, Proc. Nat. Acad. Sci. USA 98 (2001) 11867–11872.
[23] N. Mataga, H. Chosrowjan, Y. Shibata, F. Tanaka, Y. Nishina, K. Shiga, Dynamics and mechanisms of ultrafast fluorescence quenching reactions of flavin chromophores in protein nanospace, J. Phys. Chem. B 104 (2000) 10667–10677.
[24] T.M. Li, J.W. Hook, H.G. Drickamer, G. Weber, Effects of pressure upon the fluorescence of the riboflavin binding protein and its flavin mononucleotide complex, Biochemistry 15 (1976) 3205–3211.

[25] R.P. Simondsen, G. Tollin, Structure–function relations in flavodoxins, Mol. Cell Biochem. 33 (1980) 13–24.
[26] A.K. Shaw, S.K. Pal, Activity of subtilisin Carlsberg in macromolecular crowding, J. Photochem. Photobiol. B: Biol. 86 (2007) 199–206.
[27] A. Lee, S.K.Y. Tang, C.R. Mace, G.M. Whitesides, Denaturation of proteins by SDS and tetraalkylammonium dodecyl sulfates, Langmuir 27 (2011) 11560–11574.
[28] J.R. Lakowicz, Principles of fluorescence spectroscopy, Kluwer Academic/Plenum, New York, 1999.
[29] M.R. Eftink, Methods of biochemical analysis, vol. 35, John Wiley and Sons, New York, 1991.
[30] H.L. Monaco, Crystal structure of chicken riboflavin-binding protein, EMBO J. 16 (1997) 1475–1483.
[31] E.L. Gelamo, C.H.T.P. Silva, H. Imasato, M. Tabak, Interaction of bovine (BSA) and human (HSA) serum albumins with ionic surfactants: spectroscopy and modelling, Biochim. Biophys. Acta, Protein Struct. Mol. Enzymol. 1594 (2002) 84–99.
[32] J.R. Winkler, Long-range electron transfer in biology, John Wiley & Sons, Ltd, 2006.
[33] G. Markus, F. Karush, Structural effects of the interaction of human serum albumin with sodium decyl sulfate1, J. Am. Chem. Soc. 79 (1957) 3264–3269.
[34] M. Wasylewski, Binding study of riboflavin-binding protein with riboflavin and its analogues by differential scanning calorimetry, J. Protein Chem. 19 (2000) 523–528.
[35] A. Galat, Interaction of riboflavin binding protein with riboflavin, quinacrine, chlorpromazine and daunomycin, Int. J. Biochem. 20 (1988) 1021–1029.
[36] A. Galat, C. Yang, E.R. Blout, Circular dichroism study of the unfolding-refolding of a cardiotoxin from Taiwan cobra (*Naja naja atra*) venom, Biochemistry 24 (1985) 5678–5685.
[37] E.R. Blout, L. Visser, Elastase. II. Optical properties and the effects of sodium dodecyl sulfate, Biochemistry 10 (1971) 743–752.
[38] E.L. Gelamo, M. Tabak, Spectroscopic studies on the interaction of bovine (BSA) and human (HSA) serum albumins with ionic surfactants, Spectrochim. Acta A: Mol. Biomol. Spectrosc. 56 (2000) 2255–2271.
[39] S. Allen, L. Stevens, D. Duncan, S.M. Kelly, N.C. Price, Unfolding and refolding of hen egg-white riboflavin binding protein, Int. J. Biol. Macromol. 14 (1992) 333–337.
[40] J.-D. Choi, D.B. McCormick, The interaction of flavins with egg white riboflavin-binding protein, Arch. Biochem. Biophys. 204 (1980) 41–51.
[41] B. Valeur, J.C. Brochon, New trends in fluorescence spectroscopy, Springer Press, Berlin, 2001.